

# Multiple Binding Modes of Anticancer Drug Actinomycin D: X-ray, Molecular Modeling, and Spectroscopic Studies of d(GAAGCTTC)<sub>2</sub>-Actinomycin D Complexes and Its Host DNA

Shigehiro Kamitori and Fusao Takusagawa\*

Contribution from the Departments of Chemistry and Biochemistry, University of Kansas, Lawrence, Kansas 66045-0046

Received March 22, 1993\*

**Abstract:** The antitumor drug actinomycin D intercalates into DNA and strongly inhibits RNA transcription at very low concentration. Two independent structures of d(GAAGCTTC)<sub>2</sub>-actinomycin D complexes have been determined by the X-ray single crystal diffraction method (cell dimension  $a = 69.69$ ,  $b = 61.41$ , and  $c = 54.25$  Å; space group  $F222$ ;  $R$ -factor = 0.202 at 3.0-Å resolution). The complexes have an exact 2-fold symmetry in the structure. The two independent complexes are basically identical to each other and to the complex crystallized in the space group  $C2$  [*J. Mol. Biol.* **1992**, *225*, 445-456]. Actinomycin D intercalates into the middle sequence 5'-GC-3' from the minor groove of DNA. The two cyclic depsipeptide rings lie on both sides of the minor groove and cover the four base pairs of DNA. The drug is tightly connected to the DNA at the middle portion of the molecule by forming four threonine-guanine hydrogen bonds and two additional hydrogen bonds between the N2 amino group of phenoxazine and the DNA backbone. The four threonine-guanine hydrogen bonds appear to recognize the DNA sequence (5'-GC-3'). These essential hydrogen bonds are covered with the cyclic depsipeptides which are composed of mainly hydrophobic amino acid residues. However, careful examination of the structures indicates that three independent complex structures are significantly different but are rationally related. From the analysis, actinomycin D can easily change its conformation in order to fit its cyclic depsipeptides into the topographically different minor grooves of DNA's without breaking essential drug-DNA hydrogen bonds. These complex structures provide us with an additional insight into how the structure of actinomycin D has been effectively designed to bind tightly to various DNA. It is very rare that single crystal X-ray diffraction studies find three different modes for a drug to bind to the same DNA sequence. The structural data gained will be quite useful to interpret the multiple conformations of DNA-drug complexes observed by NMR studies and/or produced by the molecular mechanics and dynamics simulations. The sequence specificity of AMD is now rationally explained with the three different structures of the complex. Two independent structures of the host DNA, d(GAAGCTTC)<sub>2</sub>, have also been determined by the X-ray diffraction method (cell dimension  $a = b = 70.54$ ,  $c = 53.30$  Å; space group  $R3$ ;  $R$ -factor = 0.212 at 3.0-Å resolution). Both double-stranded DNA molecules adopt a canonical A-form DNA structure and have quite similar conformations. In both DNA's, the middle sequence, 5'-GC-3', which is the intercalation site of actinomycin D, is slightly unwound and opened up, suggesting that the host DNA takes an inherently favorable conformation for drug intercalation. A hypothetical binding process of actinomycin D has been proposed on the basis of the crystal structures of the DNA-actinomycin D complex and its host DNA. Simple molecular modeling and UV/vis spectroscopic studies have been utilized to further investigate the nature of actinomycin D. The results suggest that actinomycin D can bind intercalatively not only to B-form DNA but also to A-form DNA.

## Introduction

A group of compounds called intercalators bind intercalatively to DNA and interrupt RNA synthesis (transcription) and/or DNA synthesis (replication). Some intercalators have been used as anticancer drugs and others are carcinogens. There are several important questions to be answered in order to understand the biological activities of useful intercalators. Some of the questions are how intercalators bind to DNA, how intercalators distort DNA structures, and how intercalators recognize the binding sequence. Three-dimensional structures of DNA-drug complexes are informative enough to answer these questions. Although the structure determined by the X-ray single crystal diffraction method represents, in most cases, only one possible conformation of the molecule, this method is one of the most powerful techniques to obtain reliable and detailed three-dimensional structures of DNA-drug complexes. For this reason, the crystal structures of the complexes between DNA (hexanucleotide) and antracycline

intercalators daunomycin,<sup>1-5</sup> adriamycin,<sup>3</sup> nogalamycin,<sup>6-9</sup> and their derivatives<sup>10,11</sup> have been determined at atomic resolution. The DNA complexes of bis-intercalators triostin A,<sup>12-15</sup> echi-

(1) Quigley, G. J.; Wang, A. H.-J.; Ughetto, G.; van der Marel, G. A.; van Boom, J. H.; Rich, A. *Proc. Natl. Acad. Sci. U.S.A.* **1980**, *77*, 7204-7208.

(2) Wang, A. H.-J.; Ughetto, G.; Quigley, G. J.; Rich, A. *Biochemistry* **1987**, *26*, 1152-1163.

(3) Frederick, C. A.; Williams, L. D.; Ughetto, G.; van der Marel, G. A.; van Boom, J. H.; Rich, A.; Wang, A. H.-J. *Biochemistry* **1990**, *29*, 2538-2549.

(4) Moore, M. H.; Hunter, W. N.; d'Estaintot, B. L.; Kennard, O. *J. Mol. Biol.* **1989**, *206*, 693-705.

(5) Nunn, C. M.; Meervelt, L. V.; Zhang, S.; Moore, M. H.; Kennard, O. *J. Mol. Biol.* **1991**, *222*, 167-177.

(6) Liaw, Y.-C.; Gao, Y.-G.; Robinson, H.; van der Marel, G. A.; van Boom, J. H.; Wang, A. H.-J. *Biochemistry* **1989**, *28*, 9913-9918.

(7) Gao, Y.-G.; Liaw, Y.-C.; Robinson, H.; Wang, A. H.-J. *Biochemistry* **1990**, *29*, 10307-10316.

(8) Williams, L. D.; Egli, M.; Gao, Q.; Bash, P.; van der Marel, G. A.; van Boom, J. H.; Rich, A.; Frederick, C. A. *Proc. Natl. Acad. Sci. U.S.A.* **1990**, *87*, 2225-2229.

(9) Egli, M.; Williams, L. D.; Frederick, C. A.; Rich, A. *Biochemistry* **1991**, *30*, 1364-1372.

(10) Williams, L. D.; Egli, M.; Ughetto, G.; van der Marel, G. A.; van Boom, J. H.; Quigley, G. J.; Wang, A. H.-J.; Rich, A.; Frederick, C. A. *J. Mol. Biol.* **1990**, *215*, 313-320.

\* To whom correspondence should be addressed.

\* Abstract published in *Advance ACS Abstracts*, April 1, 1994.

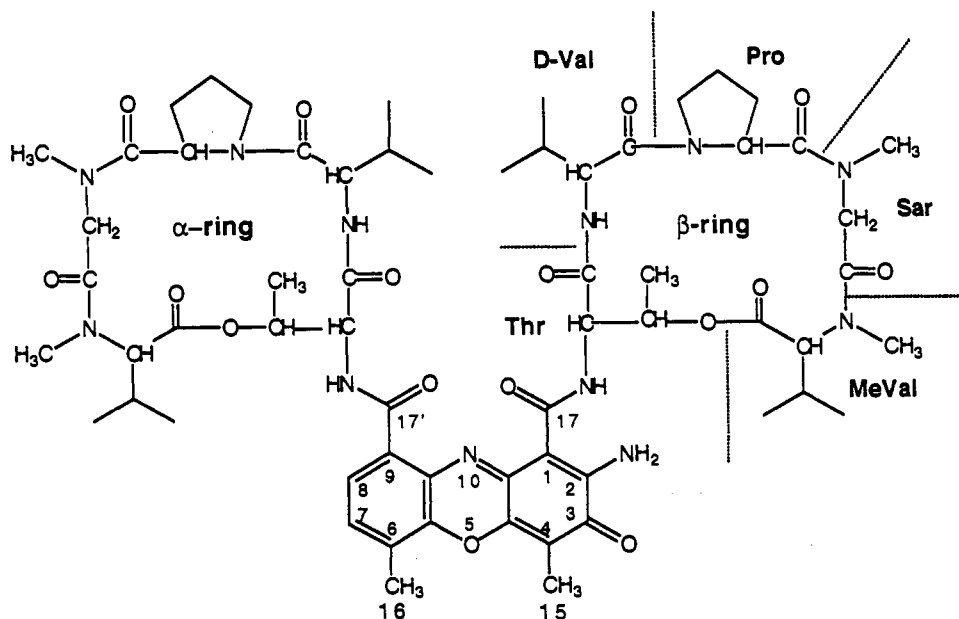


Figure 1. Molecular structure actinomycin D (AMD).

nomycin,<sup>13</sup> and ditercalinium<sup>16</sup> have been also investigated by X-ray analyses. These structures showed many interesting DNA–drug interactions and geometrical features of the DNA–drug complexes at the atomic level. However, structural changes of DNA by the drug intercalation still could not be sufficiently observed because two drug molecules intercalate at both ends of the DNA fragment. Therefore, the crystal structure of a DNA–drug complex, in which a drug intercalates between the middle base pairs of a relatively long DNA fragment (hexamer or more), has been sought as a more practical model for biological systems.

Actinomycin D (AMD) is a potent antitumor agent; however, its clinical usefulness is limited by its extreme cytotoxicity. It binds to DNA intercalatively with a relatively high binding constant ( $2.3 \times 10^6 \text{ M}^{-1}$ )<sup>17</sup> compared to those of the simple intercalators and selectively inhibits DNA-directed RNA synthesis.<sup>18,19</sup> Although AMD inhibits DNA replication, its activity is approximately 1/100 of the RNA inhibitory activity.<sup>49</sup> On the other hand, well-known anticancer drugs such as daunomycin and adriamycin bind intercalatively to DNA and equally inhibit both transcription and replication of DNA. The antitumor activity of AMD has been believed to be due to its selective inhibition of transcription. As shown in Figure 1, AMD is composed of a phenoxazone ring as an intercalating part and two cyclic pentadepsipeptides as DNA minor groove binding part. The drug has an approximate 2-fold symmetry around the N10–O5 line of the phenoxazone ring. AMD is a relatively complex molecule in comparison with daunomycin and adriamycin, which are composed of a chromophore and a small amino sugar. This complex structure of AMD should be closely related to its selective RNA

inhibitory activity and relatively high DNA binding capability. Thus, the DNA binding mode of AMD should be quite different from those of daunomycin and adriamycin, which cause little distortion of the DNA structures.<sup>1–5</sup>

In 1971, Sobell and co-workers proposed a DNA binding model of AMD based on the X-ray structure of the complex between AMD and deoxyguanosine.<sup>20,21</sup> In their model, AMD intercalates between the 5'-GC-3' base pairs of d(ATGCAT)<sub>2</sub> from the minor groove. The model has a pseudo-2-fold symmetry around the N10–O5 axis of the phenoxazone ring, including the DNA fragments. The threonine residues in the two cyclic depsipeptides of AMD bind symmetrically to the two guanine residues at the intercalation site through four hydrogen bonds which determine 5'-GC-3' as the binding sequence of AMD. This model of DNA–AMD interactions has been generally accepted since numerous physical measurements on DNA–AMD complexes have been in agreement with the model.<sup>17</sup> Recent molecular mechanics and dynamics simulations<sup>22</sup> and a 2D-NMR study<sup>23</sup> also support the model though some details do not precisely agree with each other. AMD was cocrystallized with the preferred binding sequence d(GC)<sub>2</sub>, but it did not form an intercalated structure.<sup>24</sup> In the structure, sequence specific hydrogen bonds have been found between threonine residues of AMD and guanine residues of DNA, but the other interactions between AMD and DNA have been unclear. Recently, we have determined the crystal structure of the complex between d(GAAGCTTC)<sub>2</sub> and AMD crystallized in the space group C2,<sup>25</sup> in which AMD intercalated between the middle 5'-GC-3' base pairs. This crystal structure not only confirmed Sobell's intercalation model but also revealed many interactions between DNA and AMD as well as structural changes of the DNA by intercalation of AMD. Unlike Sobell's model, the DNA–AMD complex does not have an exact 2-fold symmetry; *i.e.*, the DNA helix is unwound asymmetrically at the intercalation site, the two cyclic depsipeptides take different conformations, and they interact differently with the minor groove of DNA.

Here we report two additional structures of d(GAAGCTTC)<sub>2</sub>–AMD complexes which are significantly different from each other

(11) Cirilli, M.; Bachechi, F.; Ughetto, G. *J. Mol. Biol.* **1992**, *230*, 878–889.

(12) Wang, A. H.-J.; Ughetto, G.; Quigley, G. J.; Hakoshima, T.; van der Marel, G. A.; van Boom, J. H.; Rich, A. *Science* **1984**, *225*, 1115–1121.

(13) Ughetto, G.; Wang, A. H.-J.; Quigley, G. J.; van der Marel, G. A.; van Boom, J. H.; Rich, A. *Nucleic Acids Res.* **1985**, *13*, 2305–2323.

(14) Quigley, G. J.; Ughetto, G. A.; van der Marel, G. A.; van Boom, J. H.; Wang, A. H.-J.; Rich, A. *Science* **1986**, *232*, 1255–1258.

(15) Wang, A. H.-J.; Ughetto, G.; Quigley, G. J.; Rich, A. *J. Biomol. Struct. Dyn.* **1986**, *3*, 319–342.

(16) Gao, Q.; Williams, D.; Egli, M.; Rabinovich, D.; Chen, S.-L.; Quigley, G. J.; Rich, A. *Proc. Natl. Acad. Sci. U.S.A.* **1991**, *88*, 2422–2426.

(17) Meienhofer, J.; Atherton, E. *Structure-Activity Relationship among the Semisynthetic Antibiotics*; Perlman, D., Ed.; Academic Press, Inc.: New York, 1977; pp 427–529.

(18) Goldberg, J. H.; Friedman, P. A. *Annu. Rev. Biochem.* **1971**, *40*, 775–810.

(19) Kersten, H.; Kersten, W. *Inhibitors of Nucleic Acid Synthesis*; Springer Verlag: Berlin, 1974; pp 40–66.

(20) Sobell, H. M.; Jain, S. C.; Sakore, T. D.; Nordman, C. E. *Nature, New Biol.* **1971**, *231*, 200–205.

(21) Sobell, H. M.; Jain, S. C. *J. Mol. Biol.* **1972**, *68*, 21–34.

(22) Creighton, S.; Rudolph, B.; Lybrand, T.; Singh, U. C.; Shafter, R.; Brown, S.; Kollman, P. *J. Biomol. Struct. Dyn.* **1989**, *6*, 929–969.

(23) Liu, X.; Chen, H.; Patel, D. J. *J. Biomol. NMR* **1991**, *1*, 323–347.

(24) Takusagawa, F.; Dabrow, M. H.; Neidle, S.; Berman, H. M. *Nature* **1982**, *296*, 466–469.

(25) Kamitori, S.; Takusagawa, F. *J. Mol. Biol.* **1992**, *225*, 445–456.

**Table 1.** Crystallographic and Refinement Data of the DNA-AMD Complex and Its Host DNA

	DNA-AMD complex	host DNA
molecular formula	(C <sub>78</sub> H <sub>92</sub> N <sub>30</sub> P <sub>7</sub> O <sub>46</sub> ) <sub>2</sub> C <sub>62</sub> H <sub>86</sub> N <sub>12</sub> O <sub>16</sub>	(C <sub>78</sub> H <sub>92</sub> N <sub>30</sub> P <sub>7</sub> O <sub>46</sub> ) <sub>2</sub>
space group	F222	R3
<i>a</i> (Å)	69.69	70.54
<i>b</i> (Å)	61.41	70.54
<i>c</i> (Å)	54.25	53.30
no. of formula in asymmetric unit	1 (2 halves)	2
crystal size (mm)	0.3 × 0.3 × 0.4	0.5 × 0.5 × 0.7
resolution (Å)	8.0–3.0	10.0–3.0
no. of unique reflns measured	1268 (100% of possible)	1928 (93% of possible)
no. of reflns	1016 ( <i>F</i> <sub>0</sub> > 2.0σ( <i>F</i> <sub>0</sub> ))	1035 ( <i>F</i> <sub>0</sub> > 1.5σ( <i>F</i> <sub>0</sub> ))
no. of solvent molecules	96	140
<i>R</i> -factor	0.202	0.212
rms deviations from ideal bond distances (Å)	0.037	0.039
bond angles (deg)	5.9	6.4

and are also different from the structure crystallized in the space group C2<sup>25</sup> but are also rationally related to each other. The structure of the host DNA, d(GAAGCTTC)<sub>2</sub>, is also described here along with simple molecular modeling and UV/vis spectroscopic studies on the DNA-AMD complex.

### Experimental Section

**Crystallization.** The octanucleotide d(GAAGCTTC) was synthesized by using a Biosearch 8600 automated DNA synthesizer and purified by the reverse-phase HPLC method using a C18 reverse-phase column. AMD was purchased from Sigma and used without further purification. A typical crystallization mixture for the DNA-AMD complex contains 2.0 mM oligonucleotide, 10 mM MgCl<sub>2</sub>, 20 mM cacodylate buffer (pH 7.0), 2.0 mM spermine tetrachloride, 1.5 mM AMD, and 7.5% (v/v) 2-methyl-2,4-pentanediol (MPD). The solution was equilibrated with 15% (v/v) MPD at 4 °C. Crystals with several different habits were grown after 2 weeks. The crystals of C2 form reported previously<sup>25</sup> have also grown under the same conditions. The host DNA, d(GAAGCTTC)<sub>2</sub>, was crystallized under the same conditions except for excluding AMD.

**Data Collection.** Crystals of the DNA-AMD complex diffracted at up to 3.0-Å resolution at room temperature and decayed relatively quickly under X-ray exposure. Thus, the intensity data were measured at low temperature (–150 °C). A crystal of the DNA-AMD complex (0.3 × 0.3 × 0.4 mm) was mounted on the top of a thin glass fiber and instantly frozen under the nitrogen stream (–150 °C) on a Rigaku AFC5R X-ray diffractometer with monochromated Cu Kα radiation. Diffraction data were measured to a resolution of 3.0 Å, using the ω–2θ scan mode. Although the crystal did not decay with X-ray exposure through the entire period of data measurement, cooling the crystal did not improve the data resolution. The systematic absences of the reflections indicate the space group to be F222, which is different from the C2 reported previously.<sup>25</sup>

Although most octanucleotides whose structures have been determined diffracted well (~2.0-Å resolution),<sup>30</sup> the crystals of host DNA diffracted only up to 3.0-Å resolution. A 0.5- × 0.5- × 0.7-mm crystal of the host DNA was sealed in a glass capillary with a droplet of mother liquor, and the capillary was mounted on the same diffractometer. Diffraction intensity data were collected to a resolution of 3.0 Å, using the ω scan mode at 22 °C. The systematic absences of the reflections indicate the space group to be R3. *L*<sub>p</sub> and empirical absorption corrections were applied to both intensity data. Crystallographic experimental details are given in Table 1.

**Structure Determination and Refinement of the DNA-AMD Complex.** The Patterson map of the DNA-AMD complex clearly suggested that the base pairs were stacked along the *b*-axis. The length of the base staking axis (*b* = 61.41 Å) is the same as the *b*-axis (62.09 Å) of the crystal structure of the DNA-AMD complex crystallized in the C2 form. These characteristic features of the Patterson map and the cell dimension indicated that the complexes were stacked along the *b*-axis to form a pseudocontinuing helix as seen in the C2 form. Furthermore when the unit cell of the F222 form was superimposed on the cell of the C2 form, the crystallographic 2<sub>1</sub> axes in both cells were roughly overlapped with each other as shown in Figure 2 (A). Thus, molecular packing in the F222 unit cell was considered to be quite similar to that found in the C2 form. The complexes in the F222 cell are required to possess exact 2-fold symmetry since the crystallographic 2-fold axis must pass through the center of the complex. Thus, Sobell's model which has an exact 2-fold symmetry was superimposed on the structure of the C2 form, then the

crystal structure of the C2 form was transferred into the F222 form cell. In the F222 cell, the 2-fold axis along the *c*-axis coincides approximately with the 2-fold axis of Sobell's model. The initial crystal structure described here contains two independent complexes which have an exact 2-fold symmetry in their structures. A single-stranded DNA and a half of the AMD divided through the O5–N10 line are crystallographically independent in each complex. The N2 amino group and O3 quinoid oxygen attached to the phenoxazone ring are disordered by 50–50% at both sides of the ring. This model structure was refined and confirmed as described below.

Initially, each independent complex was treated as a rigid body, and the positional parameter along the *c*-axis (*z*) and the rotational parameter around the 2-fold axis (*φ*<sub>2</sub>) were varied using 8.0–4.0-Å resolution data (468 reflections) to give the *R*-factor of 0.49. Then the model was divided into several small rigid groups, namely base pairs, sugar and phosphate moieties, and the rigid body parameters of the groups were refined by the program X-PLOR,<sup>26,27</sup> to reduce the *R*-factor to 0.36. The structure was further refined using 8.0–3.0-Å resolution data by the POSITIONAL protocol of X-PLOR. During the refinement, the 2*F*<sub>0</sub>–*F*<sub>c</sub> electron density maps were periodically computed and were inspected on a graphics workstation using the FRODO graphics system.<sup>28,29</sup> Solvent molecules were gradually introduced in the structure. After repeating this procedure several times and adding 96 solvent molecules, the structure was refined to give the *R*-factor of 0.202 for 8.0–3.0-Å resolution data. In order to confirm the structure determined at 3.0-Å resolution, several omit maps were calculated, as has been applied in structure analysis of the C2 form.<sup>25</sup> The omit maps of phenoxazone rings, depsiptide rings, and base pairs and phosphate groups showed significant and clear electron density, suggesting that the structure has been determined correctly. A typical omit map of the phenoxazone ring is illustrated in Figure 3 (A), and the other omit maps are deposited along with crystallographic data in the supplementary material.

**Structure Determination and Refinement of Host DNA.** The volume of the asymmetrical unit (25 520 Å<sup>3</sup>) of the host DNA suggested that two double-stranded DNA's are in an asymmetric unit. Most octanucleotides whose structures have been determined crystallized in the hexagonal (*P*<sub>6</sub><sub>1</sub> or *P*<sub>6</sub><sub>1</sub>22) or the tetragonal (*P*<sub>4</sub><sub>3</sub>2<sub>1</sub>2) form.<sup>30</sup> Therefore, the trigonal cell (*R*3), which was not preceeded for an octanucleotide, was compared with known hexagonal and tetragonal cells in order to find similarities. As shown in Figure 2 (B), the corners of the hexagonal cell (6<sub>1</sub>-axes) overlap approximately with the 3-fold axes of the trigonal cell. Careful consideration of the space group *R*3 suggests that the *R*3 symmetry elements can generate a molecular packing similar to that found in the *P*<sub>6</sub><sub>1</sub> cell as shown in Figure 2 (B). There is a pseudo-6<sub>1</sub> symmetry relation between the two independent DNA's. As an initial model, an artificial crystal structure of the host DNA in the *P*<sub>6</sub><sub>1</sub> cell was generated using the d(GGGATCCC)<sup>31</sup> structure deposited in the Protein Data Bank. The 6<sub>1</sub>-axis of the model structure was placed on the 3-fold axis of the trigonal

(26) Brünger, A. T.; Kriyan, J.; Karplus, M. *Science* **1987**, *235*, 458–460.(27) Brünger, A. T. *X-PLOR 3.1. A System for X-ray Crystallography and NMR*; Yale University Press: New Haven & London, 1993.(28) Jones, T. A. *Methods Enzymol.* **1985**, *115*, 157–171.(29) Cambillau, C.; Horjales, E. *J. Mol. Graphics* **1987**, *5*, 174.(30) Dickerson, R. E. *Methods Enzymol* **1992**, *211*, 67–110.(31) Lauble, H.; Frank, R.; Bloecker, H.; Heinemann, U. *Nucleic Acids Res.* **1988**, *16*, 7799–7816.

(32) Johnson, C. K. ORTEP2. Report ORNL-5138; Oak Ridge National Laboratory: Oak Ridge, TN, 1976.

(33) Dickerson, R. E. *Nucleic Acids Res.* **1989**, *17*, 1797–1803.

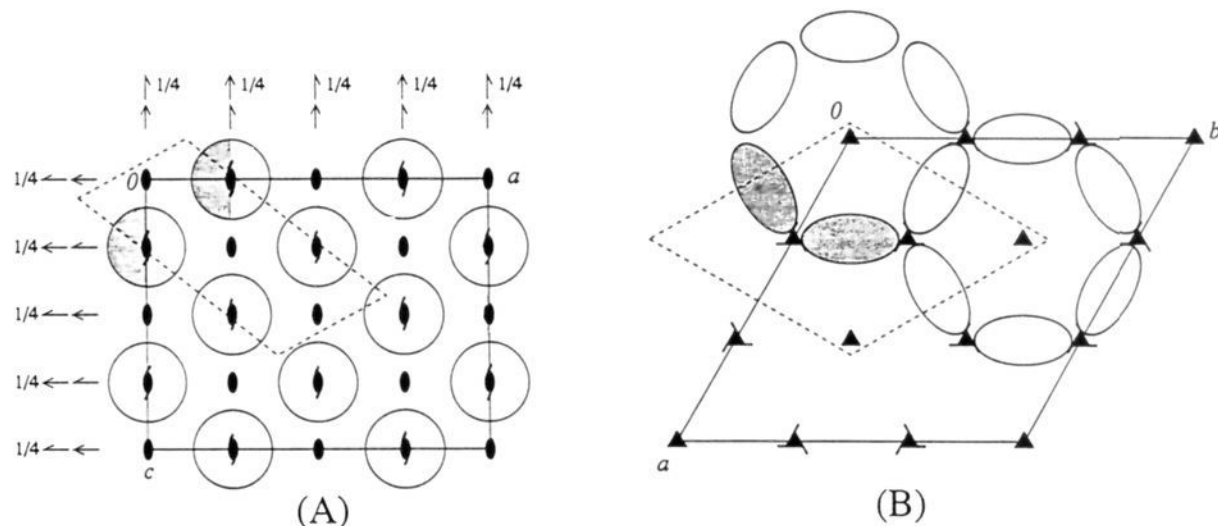


**Figure 2.** Schematic diagrams of crystal packings of the DNA-AMD complex and host DNA. Crystallographically independent regions are shaded. (A) The DNA-AMD complex viewed down the *b*-axis. Circles represent DNA-AMD complexes whose helical axes are parallel to the *b*-axis. Each complex has an exact 2-fold symmetry; *i.e.*, the 2-fold axis passes through the N10-O5 line of the phenoxazone ring of AMD. The unit cell of the DNA-AMD complex crystallized in the space group *C*2 ( $a = 51.37$ ,  $b = 62.09$ , and  $c = 25.04$  Å;  $\beta = 113.8^\circ$ )<sup>25</sup> is drawn with dashed lines to superimpose on the *F*222 cell. Locations of the 2<sub>1</sub>-axes along the *b*-axis in both unit cells agree completely with each other. (B) The crystal structure of host DNA containing two crystallographically independent double-stranded DNA's in an asymmetric unit. Each ellipsoid represents a double-stranded helix whose axis is approximately parallel to the *ab*-plane of the unit cell. The hexagonal unit cell (*P*6<sub>1</sub>) of d(GGGATCCC)<sub>2</sub> ( $a = b = 46.83$  Å,  $c = 44.49$  Å)<sup>31</sup> is drawn with dashed lines to superimpose on the *R*3 cell. Locations of the 3-fold axis of the *R*3 cell and the 6<sub>1</sub>-axis of the *P*6<sub>1</sub> cell are very close to each other, suggesting that the trigonal form belongs to the hexagonal form found in many octanucleotide structures.

cell, and then the DNA's were rotated around the *a*-axis by 5° steps. At each step, the structure was varied by treating each DNA molecule as a rigid group (two groups), using 139 reflections (10.0–4.0 Å,  $F_o > 3.0 \sigma(F_o)$ ), to give a global minimum of *R*-factor = 0.39. The model was then refined by treating each base pair and the sugar and phosphate moieties as rigid groups, decreasing the *R*-factor to 0.31 with the same reflections. The structure was further refined with the same procedure applied to the DNA-AMD complex using 10.0–3.0-Å resolution data. The current *R*-factor is 0.212. The omit map of the G4–C13 base pair is shown in Figure 3 (B), and the other maps are deposited as supplementary material.

**Molecular Modeling of Longer DNA-AMD Complexes.** Since the bases of both ends of the octamer are affected by crystal packing forces, those bases were eliminated from the structures of DNA-AMD complexes. Then three end base pairs of either A-form DNA or B-form DNA 11-mers were fitted on the three end base pairs of the hexamer structure derived from complexes. After least-squares fitting, the three end base pairs of the 11-mer were cut off to make the 8-mer DNA. Two model 8-mers were connected at both ends of the 6-mer DNA-AMD complex to give an initial 22-mer DNA-AMD complex for molecular dynamics and mechanics calculations. The initial model subjected to solvated dynamics was solved with the "BOX" option in AMBER with a shell of at least 7 Å (approximately 4000 water molecules). The solvent was then equilibrated at 200 K by fixing the solute (nucleic acid and AMD) molecules *via* harmonic potentials to their original positions. An initial 500-step minimization was performed followed by 2 ps of dynamics with a 4-kcal positional restraint on the solute and an additional 2 ps with a 1-kcal restraint. The entire system was then minimized for 1000 steps of molecular mechanics. All calculations were done with a 9-Å cutoff.

All of the calculations were performed on an IBM RISC-6000/550 workstation. Visualization and model building were done using FRODO.<sup>28,29</sup> Atomic charges and force field parameters for the nucleic acid portion of the system were taken from the standard AMBER distribution.<sup>35</sup> Charges for the nonstandard amino acids (Sarcosine and Me-Valine), peptide lactone, and chromophore were calculated with the electrostatic potential (ESP)<sup>50</sup> enhancements to MOPAC 5.5<sup>51</sup> using

AM1<sup>52</sup> optimized model tripeptides (Gly-Xxx-Gly) and a small phenoxazone derivative. Bond distance, angle, and torsion angle parameters for AMD were adjusted to reproduce the molecule in the crystal structure of AMD.<sup>34</sup> Charges on the phosphate groups were balanced by the addition of a single sodium ion to each with AMBER's automatic counterion generation capability.

**Measurement of Difference Spectra.** The dodecanucleotides d(GGGAAGCTTCCC) and r(GGG)d(AAGCTT)r(CC)d(C) were synthesized by using a Cruachem PS-250 DNA synthesizer using the protocol provided from the company. After the deprotection procedure, the crude nucleotides were purified by a reverse-phase HPLC using the C<sub>18</sub> columns. Oligonucleotide solutions (4.0 mM) were prepared from the total OD<sub>260</sub> of purified oligonucleotides and the extinction coefficient,  $\epsilon_{260}$ , of each base (8.8 for T, 7.3 for C, 11.7 for G, and 15.4 for A in cm<sup>2</sup>/μM). Calf thymus DNA solution (12 mg/mL) was prepared by weighting the DNA. The actinomycin D solutions (20 μM) were prepared to give 0.490 absorbance at 440 nm. UV/vis absorption spectra were measured on a Shimadzu UV-160 double beam spectrometer. A 1.0-mL volume of drug solution (20 μM) in 10 mM phosphate buffer (pH 7.0) was added to the sample and reference cuvettes, and the base line of the double beam spectrometer was determined with these two cuvettes. A 10-μL volume of oligonucleotide, d(GGGAAGCTTCCC), r(GGG)d(AAGCTT)r(CC)d(C), or calf thymus DNA, was added to the sample cuvette (concentration of oligonucleotides and calf thymus DNA should be 40 μM and 120 μg/mL, respectively), while the same amount of water was added into the reference cuvette. Then, difference spectra were measured at this condition. To confirm the difference spectra, the melting point spectra of DNA and RNA-DNA-RNA mixtures were measured under the same conditions. Both spectra showed that oligonucleotides were formed as double strands at 20 °C.

## Results and Discussion

**Overall Structure of the Complex.** Precise conformational details, accurate hydrogen-bond geometry, contact distances, and features such as the positions of water molecules, all of which may be significant for complete understanding of the DNA-AMD interaction, will be visible only at higher resolution. The structure determined at around 3.0-Å resolution, however, provides relatively accurate positions and orientations of rigid groups, such as bases and base pairs. The overall conformations of the DNA backbone and cyclic peptide rings are also visible at this resolution. Intermolecular interactions, mainly hydrogen

(34) Ginell, S.; Lessinger, L.; Berman, H. M. *Bipolymers* **1988**, *27*, 843–864.

(35) Pearlman, D. A.; Case, D. A.; Caldwell, J. C.; Seibel, G. L.; Singh, U. C.; Weiner, P.; Kollman, P. A. AMBER, UCSF, Version 4.0.

(36) Chen, F.-M. *Biochemistry* **1988**, *27*, 1843–1848.

(37) Chen, F.-M. *Biochemistry* **1988**, *27*, 6393–6397.

(38) Bailey, S.; Graves, D. E.; Rill, R.; Marsch, G. *Biochemistry* **1993**, *32*, 5881–5887.

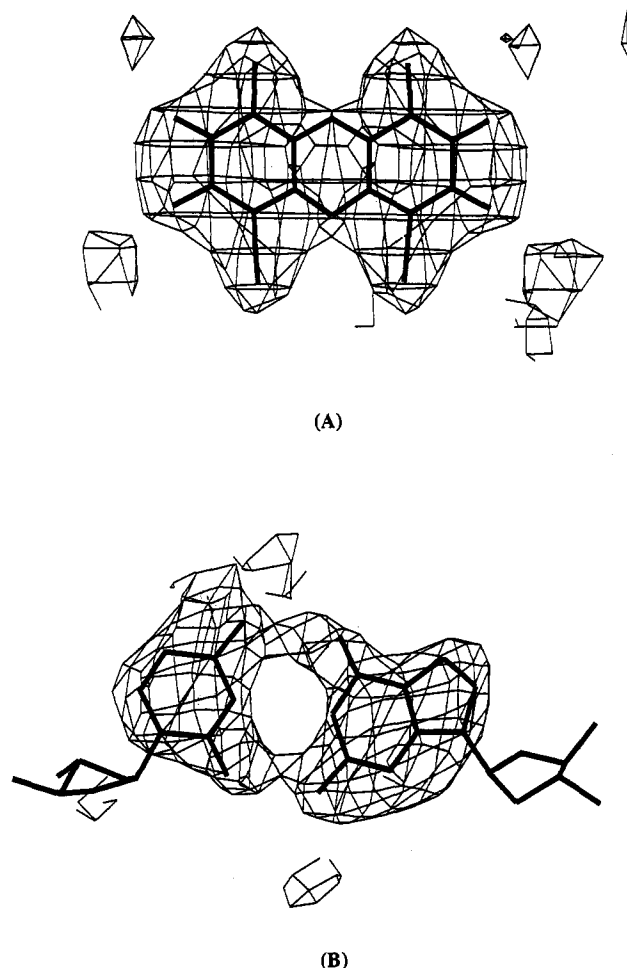


**Figure 3.** Omit maps of selected sections of the DNA-AMD complexes and the host DNA: (A) the phenoxazone ring of complex A in the DNA-AMD complex; (B) the G4-C13 base pair of DNA-1 in the host DNA. The other sections were deposited (as supplementary material). Omit maps were calculated by the following procedures: (1) the occupancy factors of omitted atoms were set to zero; (2) the structure was refined by 40 cycles of least-squares using the POSITIONAL protocol of X-PLOR;<sup>26</sup> (3) the  $F_o - F_c$  map was calculated and drawn at the contour level of  $1.25\sigma$ .

bonds and van der Waals (vdw) interactions, are distinguishable. Thus, we believe our present structure to be sufficiently well determined to address many key questions regarding DNA-AMD interactions.

Two independent complexes found in the *F222* form crystal are named complexes A and B, respectively, and the complex crystallized in the space group  $C2^{25}$  is labeled as complex C in the text. Structures of these three independent complexes are put together in the figures and tables in order to explain easily how these structures are different from each other and also how these structures are related to each other. The DNA sequence numbering is given in Figure 4.

Complexes in the three structures are stacked together to form a pseudocontinuous helix running through the crystals. Stereoscopic views of complexes A, B, and C are illustrated in Figures 4 and 5. Complex C does not have an exact 2-fold symmetry, whereas complexes A and B have an exact 2-fold symmetry around N10-O5 axis in the phenoxazone ring. Strictly speaking, AMD molecules in complexes A and B are disordered in the crystal structures since the amino group (N2) and quinoid oxygen (O3) of the phenoxazine ring break the exact 2-fold symmetry of AMD (see Figure 1). In all complex structures, AMD's intercalate into the middle sequence 5'-GC-3' from the minor groove of DNA. The two cyclic depsipeptide rings lie on both sides of the minor groove and cover the four base pairs (A3-T14, G4-C13, C5-

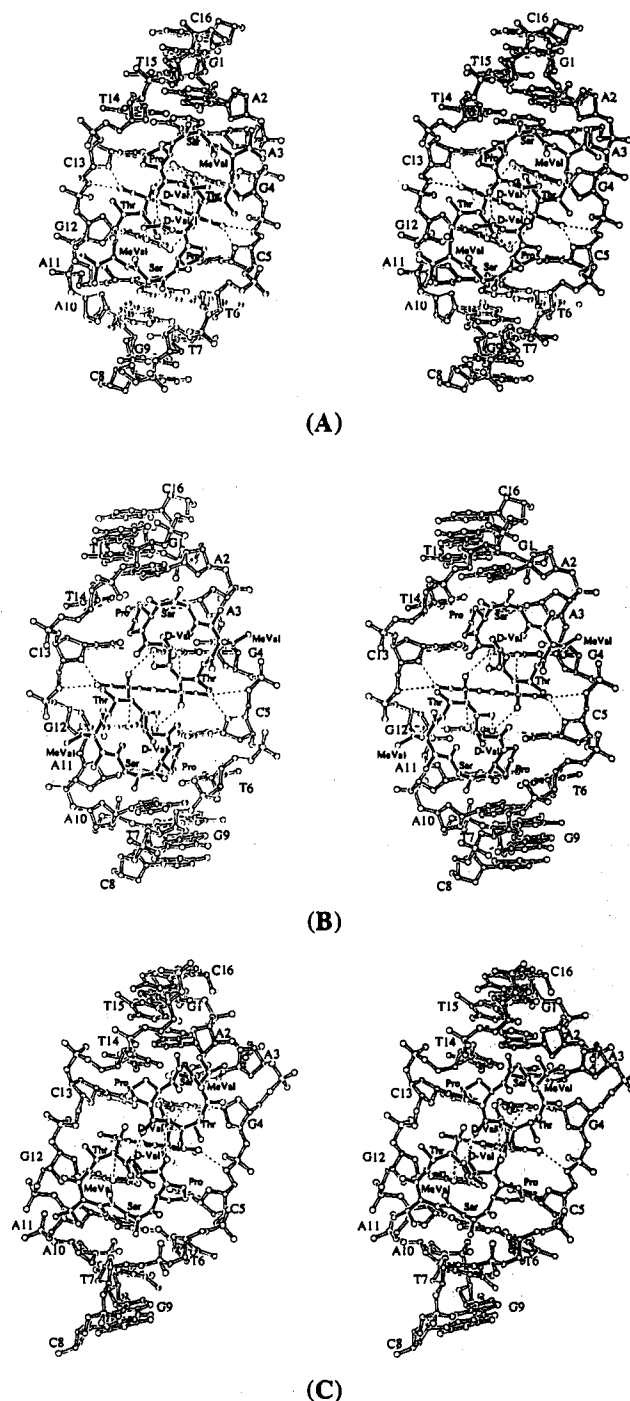
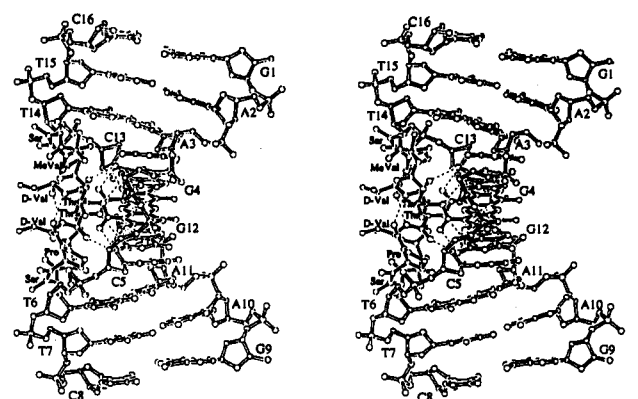


**Figure 4.** Stereo drawings of DNA-AMD complexes viewed down the minor groove of DNA: (A) complex A; (B) complex B; (C) complex C. AMD molecules are illustrated with solid bonds while the DNA has open bonds. Hydrogen bonds are also shown by dashed lines. The DNA sequence is numbered as

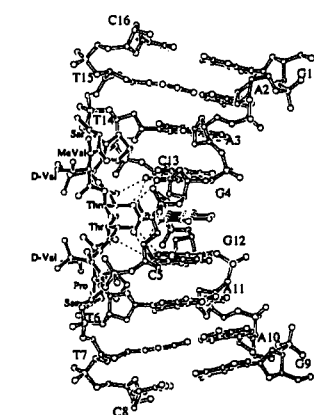
gidJA5B19b

The  $\beta$ - and  $\alpha$ -rings of AMD referred to in the text are the cyclic depsipeptides located above and below the phenoxazone ring in the figures, respectively.

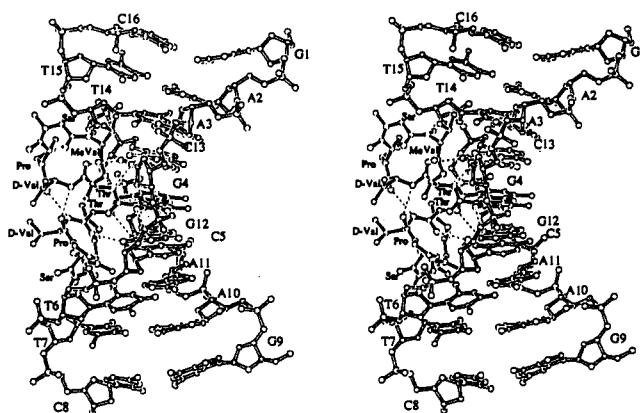
G12, and T6-A11) of DNA. AMD's are tightly connected to the DNA at the middle portion of the molecule by forming four threonine-guanine hydrogen bonds and two additional hydrogen bonds between the N2 amino group of phenoxazone and the DNA backbone. The four threonine-guanine hydrogen bonds appear to recognize the DNA sequence 5'-GC-3' as pointed out by Sobell.<sup>21</sup> These essential hydrogen bonds are covered with the cyclic depsipeptides which are constructed with mainly hydrophobic amino acid residues. To this extent, all three complexes



(A)



(B)

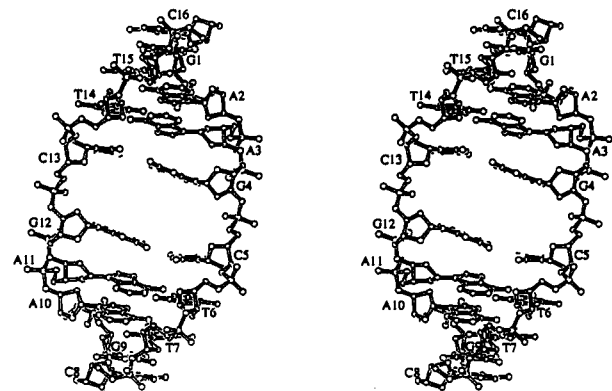


(C)

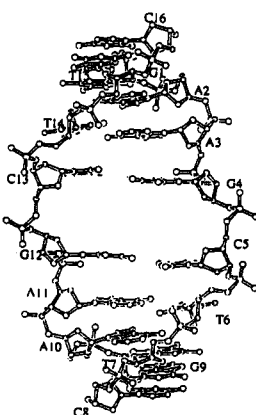
Figure 5. Stereo drawings of side views of DNA-AMD complexes in Figure 4, showing backbone conformations of DNA's.

take the same structure. However, there are several significant differences among the structures as seen in Figures 4 and 5. They are (1) the DNA minor grooves in complex B and in the  $\beta$ -ring side of complex C are wider than those in complex A and in the  $\alpha$ -ring side of complex C; (2) the cyclic depsipeptides in three complexes interact differently with the DNA minor groove; (3) stacking modes between base pairs and the phenoxazone ring are significantly different from each other; and (4) inter-ring hydrogen bonds between the D-valine residues of depsipeptide rings are observed in complexes A and C, but no such hydrogen bond is found in complex B. These differences suggest that AMD can bind differently to topologically different DNA's. It is very rare that single crystal X-ray diffraction studies find three different binding modes for a drug to the same DNA sequence.

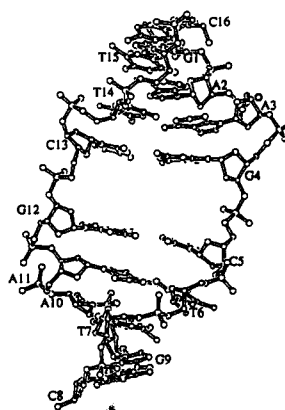
**Complexes and Noncomplexed DNA Structures.** Severely



(A)



(B)



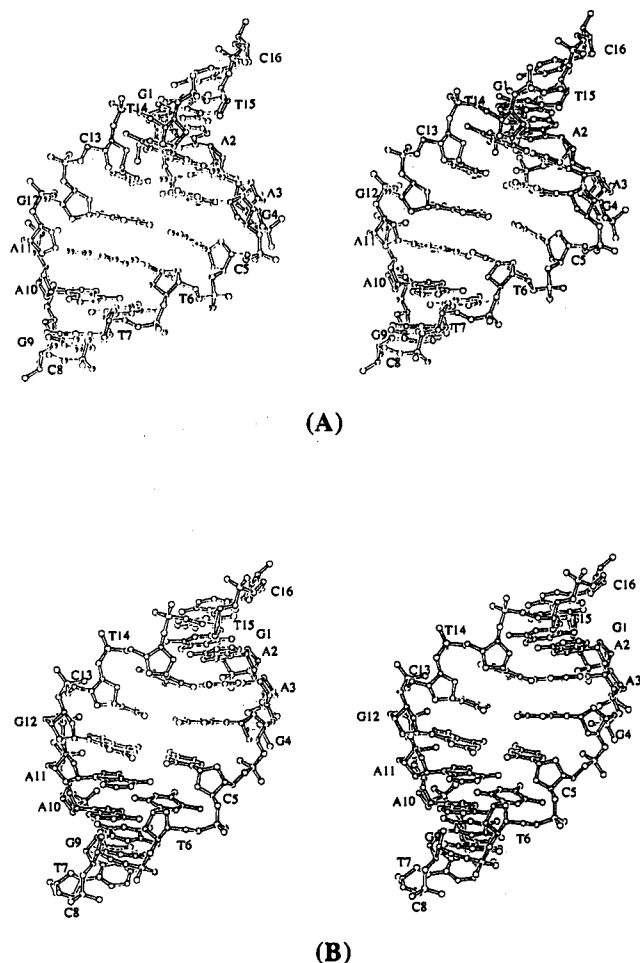
(C)

Figure 6. Stereo drawings of the complexed DNA,  $d(\text{GAAGCTTC})_2$ , viewed down the minor groove of DNA: (A) DNA in complex A; (B) DNA in complex B; (C) DNA in complex C. The DNA's have a large space between the middle base pairs where the intercalation site of AMD is.

distorted DNA structures in AMD-DNA complexes and normal DNA structures in the noncomplexed host DNA's are shown in Figures 6 and 7, respectively. Geometrical data of DNA's are listed in Table 2, and the root-mean-square (rms) deviations between two DNA's which indicate quantitatively the similarity of two DNA's, are given in Table 3.

In the complexed DNA structures, the base pair rise at the intercalation site is approximate twice those of other sites (Table 2). The mean base pair rise excluding the intercalation site is 3.4 Å in all three complex structures, which is in good agreement with the value observed in the canonical B-form DNA.<sup>30</sup> The helices are unwound very largely at the intercalation sites. Helix twist angles at the intercalation sites are 1°, 14°, and 2° for





**Figure 7.** Stereo drawings of the host DNA,  $d(\text{GAAGCTTC})_2$ , viewed down the minor groove of DNA: (A) DNA in host DNA-1; (B) DNA in host DNA-2.

complexes A, B, and C, respectively, indicating a larger unwinding is taken place in complexes A and C. Helix twist angles adjacent to the intercalation site are significantly different in the three complex structures. In complex A, the helix is tightly twisted at both sites, whereas the helix of complex B is loosened in both sites. In complex C, the helix is asymmetrically twisted, *i.e.*, one side ( $\alpha$ -ring side) is tightened and the other side ( $\beta$ -ring side) is loosened. As will be discussed later, these characteristic differences in DNA unwinding appear to correlate with the DNA-AMD interaction. It is impossible to determine the helical axes of severely distorted DNA's by using a standard method.<sup>33</sup> Since all complexes are stacked together along the crystallographic *b*-axis to form a pseudo-continuous helix, the *b*-axis is assumed to be the helical axis. The base pairs in the three complexes are all tilted from the helical axis by  $17^\circ$  in complex A,  $12^\circ$  in complex B, and  $15^\circ$  in complex C, which are in relatively good agreement with the value ( $20^\circ$ ) found in a canonical A-form DNA.<sup>35</sup> Since the rms deviation between complexed DNA and canonical B-form DNA is the smallest, a canonical B-form DNA fragment (four base pairs) was fitted on the top and bottom four base pairs in order to determine the helical axes of the top and bottom portions of the severely distorted DNA. The helical axes of two portions of DNA determined by the procedure described above make angles of  $19^\circ$  for complex A,  $14^\circ$  for complex B, and  $24^\circ$  for complex C. These values suggest that the DNA's are kinked at the intercalation site. However, since structures of DNA's are severely distorted by intercalation of AMD, the two helical axes determined from the structures will contain relatively large ambiguity. Furthermore, there is no kink if a canonical A-form DNA is used instead of a B-form DNA for the helical axes determination. Thus, it is difficult to conclude whether DNA's are kinked at the

intercalation sites from this data. Similarly, it is impossible to conclude whether the DNA's adopt the A or B conformation. As listed in Table 3, the rms deviations of the base pair atoms of the complexed DNA from the canonical A- or B-form DNA indicate that DNA's in the three complexes are neither A-form nor B-form DNA. Although the B-form DNA gives the smallest rms deviation from all complexed DNA, the differences are not significant.

Although an NMR study<sup>53</sup> has found some of the octa-nucleotides taking different conformations in solution and in the solid, the crystal structure of the host DNA,  $d(\text{GAAGCTTC})_2$ , has been determined in order to examine how the DNA structure is changed by intercalation of AMD. The crystal structure of the host DNA contains two independent double-stranded DNA's in an asymmetric unit. These two DNA's are named DNA-1 and DNA-2 and are illustrated in Figure 7. Both DNA's adopt a typical A-form conformation in the solid state. When the complexed and noncomplexed DNA structures are compared to each other, it is very clear how DNA structures are distorted by intercalation of AMD. It should be noted that simple intercalators, such as daunomycin and adriamycin, do not distort the DNA structure very much when they intercalate into DNA. In the structure of the  $d(\text{CGTACG})_2$ -daunomycin<sub>2</sub> complex,<sup>1</sup> the base pair rise at the intercalation site is quite large, but the remaining portion of the DNA structure adopts a typical B-form conformation, suggesting that the drug binds to a B-form DNA.

There are no special features on the host DNA structures except for the central G-C steps. The base pair rise at the central G-C step, which is the AMD intercalation site, is slightly larger than the mean value (Table 2), suggesting that the host DNA may take an inherently favorable conformation for drug intercalation. The helix twist angles and backbone conformations of P-O5'-C5'-C4' at the central G-C steps in both DNA's are significantly different from those of the canonical A-form DNA (twist angle =  $32^\circ$  and P-O5'-C5'-C4' = (-)gauche-trans-(+)gauche). The helices in both DNA's are significantly unwound at the central G-C steps ( $\sim 12^\circ$  for DNA-1 and  $\sim 9^\circ$  for DNA-2), and the backbone conformations of P-O5'-C5'-C4' are (-)gauche-trans-(+)gauche in the G4-C5 step of DNA-1, trans-trans-(+)gauche in the G12-C13 step of DNA-1, trans-trans-trans in the G4-C5 step of DNA-2, and trans-(-)gauche-(+)gauche in the G12-C13 step of DNA-2. Although it is hard to characterize precisely the backbone conformation at 3.0-Å resolution, similar unusual backbone conformations (such as trans-trans-trans) accompanied with unwinding of helices ( $\sim 10^\circ$ ) at the central C-G steps have been observed in several A-form DNA structures determined by high-resolution X-ray studies.<sup>39,41,43</sup> Thus, the unusual backbone conformations found in this study might be significant. If the backbone conformation of P-O5'-C5'-C4' is changed from (-)gauche-trans-(+)gauche to trans-trans-trans, lone-pair electrons of O5' will point out the minor groove from the major groove, so that the minor groove has more hydrophilic character than a canonical A-form DNA. For example, O4' and O5' atoms of cytosine C5 residue in DNA-2 create a local hydrophilic character on the minor groove surface, since the backbone conformation of the G4-C5 step is trans-trans-trans. As will be discussed later, this hydrophilic character of the G-C step may send an important signal to AMD which aids AMD in approaching the binding sequence in long DNA.

(39) Takusagawa, F. *J. Biomol. Struct. Dyn.* **1990**, *7*, 795-809.

(40) Wang, A. H.-J.; Fujii, S.; van Boom, J. H.; Rich, A. *Proc. Natl. Acad. Sci. U.S.A.* **1982**, *79*, 3968-3972.

(41) Haran, T. E.; Shakked, Z.; Wang, A. H.-J.; Rich, A. *J. Biomol. Struct. Dyn.* **1987**, *5*, 199-217.

(42) Ravinovich, D.; Haran, T. E.; Eisenstein, M.; Shakked, Z. *J. Mol. Biol.* **1988**, *200*, 151-161.

(43) Heinemann, U.; Lauble, H.; Frank, R.; Blocker, H. *Nucleic Acids Res.* **1987**, *15*, 9531-9550.

(44) Verdager, N.; Aymami, J.; Fernandez-Fornier, D.; Fita, I.; Coli, M.; Huynh-Dinh, T.; Igolen, J.; Subirana, J. A. *J. Mol. Biol.* **1991**, *221*, 623-635.

**Table 2.** Helix Twist Angles, Base pair Rise Parameters, and Base pair Inclination Angles Found in d(GAAGCTTC)<sub>2</sub>-AMD Complexes and Their Host DNA<sup>a</sup>

Helix Twist Angles (deg)									
	G1-A2	A2-A3	A3-G4	G4-C5	C5-T6	T6-T7	T7-C8	mean	
complex A	28	16	47	1	47	16	28	26	
complex B	39	34	22	14	22	34	39	29	
complex C	14	48	27	2	44	40	18	28	
DNA-1	33	39	32	20	35	33	27	31	
DNA-2	26	30	36	23	39	30	23	30	
Base Pair Rise Parameters (Å)									
	G1-A2	A2-A3	A3-G4	G4-C5	C5-T6	T6-T7	T7-C8	mean	
complex A	3.4	2.7	4.0	6.5	4.0	2.7	3.4	3.4 <sup>b</sup>	
complex B	2.6	3.5	4.0	7.0	4.0	3.5	2.6	3.4 <sup>b</sup>	
complex C	3.4	3.1	3.1	7.6	3.5	2.8	4.4	3.4 <sup>b</sup>	
DNA-1	3.0	3.0	1.6	3.9	2.2	3.7	3.1	2.9	
DNA-2	2.5	3.0	3.0	3.4	3.4	2.3	3.5	3.0	
Base Pair Inclination (deg)									
	G1-C16	A2-T15	A3-T14	G4-C13	C5-G12	T6-A11	T7-A10	C8-G9	mean
complex A	16	16	15	19	19	15	16	16	17
complex B	16	15	10	5	5	10	15	16	12
complex C	12	22	15	10	12	18	12	17	15
DNA-1	33	25	26	24	22	19	16	10	22
DNA-2	18	18	13	15	24	27	21	17	19

<sup>a</sup> The helix twist angles and base pair rise parameters are defined and calculated by the procedures recommended at the EMBO Workshop on DNA Curvature and Bending held at Churchill College in 1988.<sup>56</sup> The inclination of the base pair is defined as the angle between the helix axis of DNA and the vector perpendicular to the base pair. The helix axes of DNA-AMD complexes are assumed to be parallel to the crystallographic *b*-axis (see details in text). The helix axes of host DNA molecules were calculated by the definition of program NEWHELIX<sup>33</sup> developed by Dickerson *et al.* <sup>b</sup> These values are calculated by excluding the rise at the intercalation site (G4-C5).

**Table 3.** The rms Deviations (Å) between Two Different DNA's<sup>a</sup>

	complex A	complex B	complex C	DNA-1	DNA-2
complex A	0.00	1.70	2.08	2.07	2.30
complex B	1.70	0.00	2.12	2.13	2.51
complex C	2.08	2.12	0.00	1.97	2.24
DNA-1	2.07	2.13	1.97	0.00	1.62
DNA-2	2.30	2.51	2.24	1.62	0.00
A-DNA	1.95	2.19	1.97	1.61	1.64
B-DNA	1.77	2.00	1.82	3.74	3.92

<sup>a</sup> The least-squares fitting between two DNA structures was carried out by minimizing the value.  $M = \sum D_i^2$ , where  $D_i$  is the distance between the *i*th corresponding atoms. All non-hydrogen atoms were used in the minimization. The rms deviation is defined as  $(\sum D_i^2/n)^{1/2}$ , where *n* is the number of total atoms used for the fitting. In the DNA-AMD complexes, the top and bottom four base pair residues were independently fitted to the target fragments, respectively. Although the DNA's in complex C, DNA-1, and DNA-2 do not have an exact 2-fold symmetry, the rms deviations were calculated by the same procedures applied to the symmetrical DNA's.

The cell volume per base pair (1595 Å<sup>3</sup>) of this octamer is quite similar to those found in hexagonal structures (1590 ± 93 Å<sup>3</sup>) but different from those of the tetragonal structures (1399 ± 45 Å<sup>3</sup>).<sup>30</sup> It is quite consistent with the fact that the molecular packing in the trigonal cell is quite similar to that in the hexagonal cell. Although a relatively large crystal was used to measure the X-ray diffraction data, the crystal diffracted poorly (3.0-Å resolution) in comparison to the tetragonal and hexagonal crystals which diffracted to around 2.0-Å resolution.<sup>30</sup> Poor diffraction of the crystal suggests that the trigonal structure is a metastable structure of hexagonal form and thus it might be similar to the solution structure.

**AMD Structure.** As shown in Figure 4, there are several significant differences among the AMD molecules in the three complex structures, though structures of the three individual components, the phenoxazone ring and two cyclic depsipeptides, are quite similar in the three structures. The phenoxazone rings are planar within errors, and all six cyclic depsipeptides take a similar rectangular conformation, though some side chains are oriented in a little different direction among the three complexes.

Thus, differences in the AMD structures are mainly due to differences in the torsion angles of the N-Cα(Thr) bonds connecting the cyclic depsipeptides to the phenoxazone ring. The large cyclic depsipeptide rings are moved by a slight rotation of the N-Cα(Thr) bond, in order to fit the rings well into the minor grooves of DNA's where the topographies are different in each DNA. Such a rotation of the N-Cα(Thr) bond does not break the essential hydrogen bonds between the drug and DNA since the threonine residue moves very little in the rotation. Two cyclic depsipeptides are connected through two inter-ring hydrogen bonds between the amide groups and carbonyl oxygen atoms of the D-valine residues, which appear to reduce the mobility of the rings. These inter-ring hydrogen bonds have been found in structures of AMD itself<sup>34</sup> and all AMD-DNA complexes except for complex B. As shown in Figure 4, the long edges of the rectangle of the cyclic depsipeptides of AMD in complexes A and C are approximately parallel to the phenoxazone ring plane. The same relative orientation between the cyclic depsipeptides and phenoxazone ring is seen in the structures of d(G)<sub>2</sub>-AMD,<sup>20</sup> d(GC)<sub>2</sub>-AMD,<sup>24</sup> and AMD itself.<sup>34</sup> On the other hand, in complex B, the long edge of the rectangle of the cyclic depsipeptides is tilted by approximately 25° from the phenoxazone ring plane. As a result, two inter-ring hydrogen bonds, between the amide groups and carbonyl oxygen atoms of D-valine residues, are broken by rotations of the N-Cα(Thr) bonds in complex B. This rather large structural change in AMD should be induced in order to fit the cyclic depsipeptides into the wide and shallow DNA minor groove. In contrast, the proline residue of the β-ring in complex C appears to be forced out the wide and shallow DNA minor groove but the inter-ring hydrogen bonds are kept. In this case, probably the backbone conformations of the cyclic depsipeptide are slightly adjusted to fit the most portions into the DNA minor groove instead of breaking the inter-ring hydrogen bonds. Consequently, this cyclic depsipeptide is the most irregularly shaped rectangle of the six depsipeptides found in complexes A, B and C.

**Binding Site Geometry.** Geometries of intercalation sites are shown in Figure 8. In all structures, the phenoxazone ring intercalates between G4-C13 and C5-G12 base pairs of the DNA



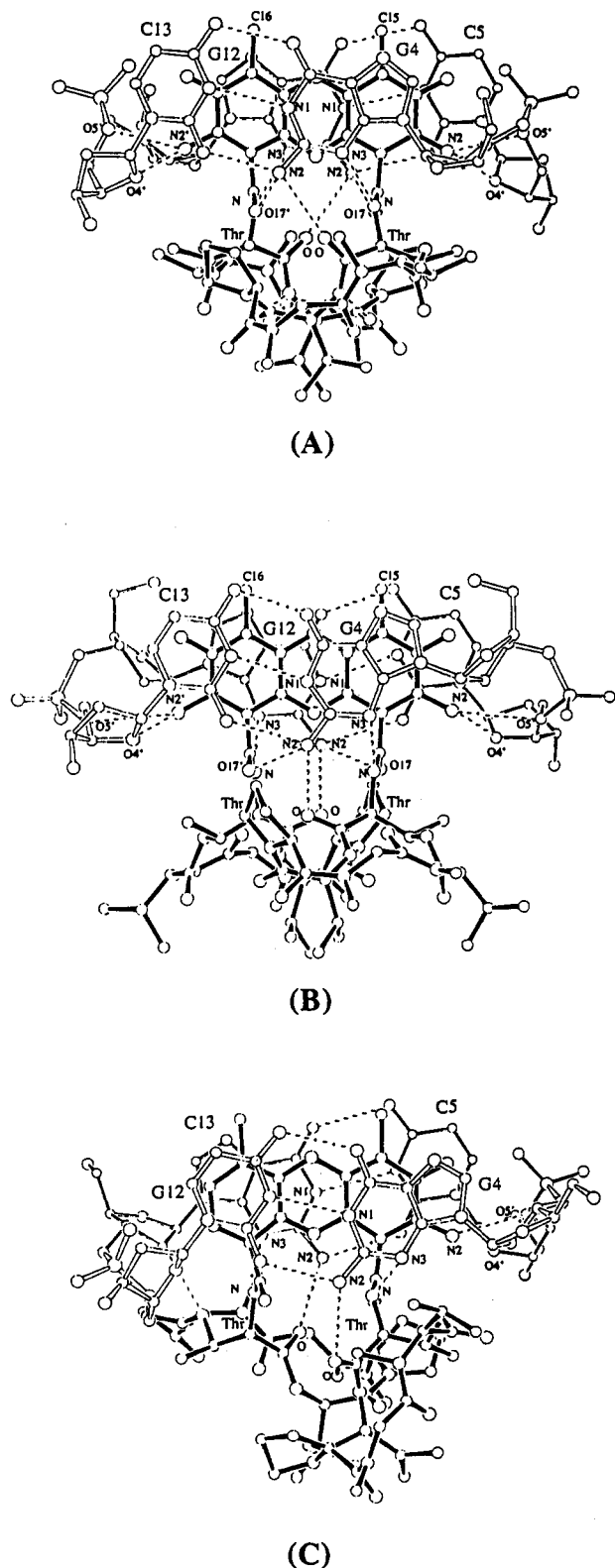


**Figure 8.** Binding site geometries of DNA-AMD complexes viewed down the phenoxazone plane. The G4 and C13 residues which are mostly above the phenoxazone ring are drawn with thick open bonds, while the C5 and G12 residues are drawn with thin open bonds. AMD molecules are drawn with thick solid bonds. The hydrogen bonds are indicated with dashed lines.

from the minor groove. The two methyl groups (C15 and C16) attached to the phenoxazone ring pass through the base pairs and come out the major groove of the DNA, which appears to play the role of anchor to prevent easy separation of AMD from the DNA.  $N2-H(G)\cdots O(Thr)$  and  $N-H(Thr)\cdots N3(G)$  hydrogen

bonds which recognize the intercalation site, 5'-GC-3', are observed in all complexes. In complexes A and B, carbonyl oxygens O17 and O17' are located at hydrogen-bonding distance with the N2 of the guanine residue. These weak hydrogen bonds may also participate in recognition of the binding sequence. In addition to these hydrogen bonds, the amino group (N2) attached to the phenoxazone ring is involved in hydrogen bonding to O4' and/or O5' of the cytosine C5 residue in all complexes. As will be discussed in later, these hydrogen bonds not only connect the drug to DNA but also play a role in initial interactions between DNA and AMD when the drug approaches a binding site. Methyl groups of threonine and *N*-methyl groups of methylvaline residues in cyclic depsipeptides are pointed to the DNA minor groove to cover the essential threonine-guanine hydrogen bonds.

As shown in Figure 8, the G-C base pairs stack on the phenoxazone ring quite differently in all these complexes. In complex A, the guanine rings of G-C base pairs overlap completely on the phenoxazone ring whereas the cytosine rings show very little overlap. On the other hand, both cytosine and guanine rings of complex B stack on the phenoxazone ring. In complex C, the guanine ring in the G12-C5 base pair overlaps dominantly on the phenoxazone ring, whereas both rings in the G4-C13 base pair stack on the phenoxazone ring. These differences in stacking patterns are well correlated with differences in helix twist angles and depsipeptide-DNA interactions.

There are significant differences in the mean helix twist angles of the central four base pairs covered by AMD ( $32^\circ$  for complex A,  $19^\circ$  for complex B, and  $24^\circ$  for complex C). In complex A, the helix appears to be unwound by twisting the intercalation site base pairs, G4-C13 and C5-G12, with  $16^\circ$  in anticlockwise and clockwise directions, respectively, without twisting the adjacent base pairs, A3-T4 and T6-A11. In other words, most unwinding motion appears to be very local and mostly absorbed at the first neighboring base pairs. On the other hand, unwinding of the helix at the intercalation site in complex B is spread over the entire helix. In complex C, the  $\alpha$ -ring side of the helix (C5  $\rightarrow$  C8) is very locally unwound, similar to what is observed in complex A, whereas the unwinding pattern of the  $\beta$ -ring side of helix (A1  $\rightarrow$  G4) is quite similar to that observed in complex B. As will be described below, a good correlation is seen between the helix unwinding pattern and the base-phenoxazone stacking pattern. When the helix is tightly wound adjacent to the intercalation sites, the guanine ring predominantly stack on the phenoxazone ring. On the other hand, when the helix is loosened adjacent to the intercalation site, both guanine and cytosine rings stack on the phenoxazone ring. Similarly when the helix is tightened between the G-C and A-T base pairs (in cases of complex A and the  $\alpha$ -ring side of complex C), the cyclic depsipeptides are fitted well into the minor groove and appear to have sufficient vdw interactions with the surface of the minor groove. On the other hand, when the helix is loosened between the G-C and A-T base pairs (in cases of complex B and the  $\beta$ -ring side of complex C), the cyclic depsipeptides are not fitted well into the minor groove. More specifically, the helix unwinding patterns can be correlated to proline-DNA interactions. The proline residues in complex A and in the  $\alpha$ -ring of complex C are located between the deoxyribose moieties of cytosine C5 and thymine T6 and appear to have sufficient vdw interacts with those moieties. The large helix twist is probably induced by deep penetration of the proline residue into the DNA minor groove. On the other hand, when the proline residue interacts weakly with DNA such as seen in complex B and in the  $\beta$ -ring of complex C, the helix was slightly loosened (unwound) adjacent to the intercalation sites. For example, the proline residue in complex B stacks with the deoxyribose moieties of T6 with vdw interactions but does not interact with cytosine C5. Similarly, the proline in the  $\beta$ -ring of complex C locates outside the DNA minor groove and thus does

not interact with any deoxyribose moiety of DNA. In these cases, the helix twist angles adjacent to the intercalation site are  $22^\circ$  for complex B and  $27^\circ$  for complex C, which are slightly smaller than the normal DNA twist angle ( $\sim 32^\circ$ ).

The helix twist, vdw interaction between the cyclic depsipeptide and the DNA minor groove, and the stacking pattern between the G-C base pair and the phenoxazone ring found in the  $\alpha$ -ring side of complex C are quite similar to those of complex B, whereas the structure at the  $\beta$ -ring side of complex C resembles the structure of complex A. Thus, complex C should be an intermediate between complex A and complex B. Since these structures have been found in the crystals, these three complexes must all be stable structures. Therefore, these structures represent the major conformations of the DNA-AMD complex.

**Binding Site Sequence.** Since each cyclic depsipeptide of AMD covers two base pairs adjacent to the intercalation site, AMD is expected to recognize a total of four base sequences. According to studies by Chen,<sup>36,37</sup> the preference of AMD binding sequences are in the order of TGCA > CGCG > AGCT  $\gg$  GGCC. However, the hydrophobic groups of sarcosine and methylvaline residues in complex C, whose structure was determined previously, pointed to the minor groove to have sufficient vdw contacts with the A-T base pairs adjacent to the intercalation site 5'-GC-3'. Thus the A or T residue, whose minor groove has more hydrophobic character than the G or C residue, is thought to be a more favorable DNA sequence adjacent to the intercalation site than the G or C residue. Moreover, when the A-T base pairs at this position were replaced with the G-C or C-G base pairs without changing the AMD structure, there were unusual short contacts between the amino group (N2) of the guanine residue and the sarcosine or methylvaline residues. Therefore, from the structure of complex C, the X and Y sequences next to the intercalation site, 5'-XGCY-3', were thought to be restricted to A or T residues.<sup>25</sup> However, in complexes A and B, the sarcosine and methylvaline residues have a few favorable vdw contacts with the base pairs. The hydrophobic groups of sarcosine and methylvaline residues interact mainly with sugar-phosphate backbones of DNA. Consequently, a moderate space is created between the depsipeptide ring and the minor groove of DNA which is large enough to fit the amino group (N2) of guanine and/or the carbonyl group (O4) of cytosine residues. Thus, in the structures of complexes A and B, replacing the A-T base pair with the G-C base pair adjacent to the intercalation site does not cause unusual short contact with AMD. If AMD binds to DNA in a similar fashion to complexes A and B in solution or *in vivo*, AMD will be able to bind to all of the four base sequences TGCA, AGCT, CGCG, and GGCC. This is supported by the recent study of the binding energy of AMD,<sup>37</sup> in which binding enthalpies of AMD to TGCA and CGCA are  $-2.5$  and  $-6.1$  kcal/mol, respectively, in spite of the TGCA binding constant ( $4.6 \times 10^6$  M $^{-1}$ ) being larger than that for CGCA ( $2.4 \times 10^6$  M $^{-1}$ ). This suggests that AMD interacts more favorably with the C-G base pair than the T-A base pairs adjacent to the 5'-GC-3' intercalation site.

**Proposed Intercalation Process of AMD.** Since AMD intercalates its phenoxazone ring from the minor groove, some plausible interactions between AMD and the minor groove of DNA are necessary for AMD to approach DNA. As proposed by Hamilton,<sup>45</sup> AMD probably approaches DNA with the negatively charged quinoid (O3) and positively charged amino group (N2) of the phenoxazone ring pointed toward the minor groove of DNA. These charged groups can interact with the positively charged amino group (N2) of guanine and negatively charged oxygen atoms (O4' and O5') in the minor groove, respectively. Several models of AMD approaching DNA have been built on the basis of the DNA-1 and DNA-2 found in this study as well as the

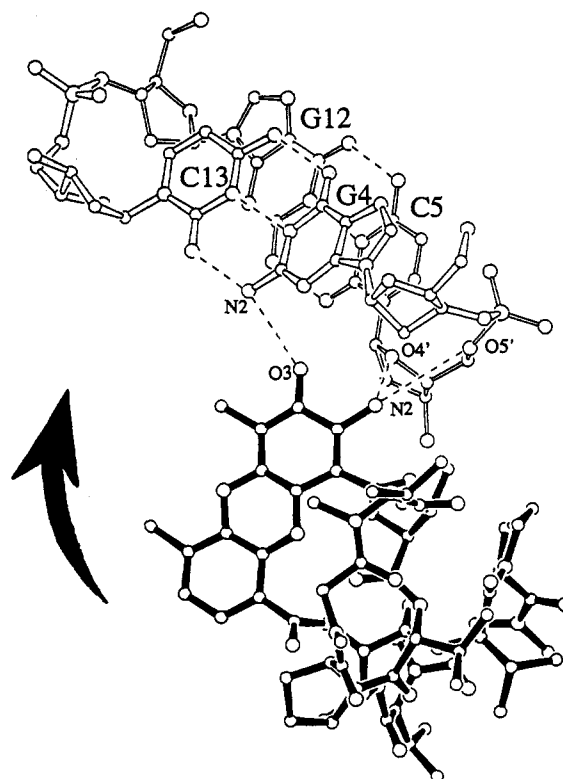


**Figure 9.** Proposed initial contact between AMD and DNA when the drug approaches the DNA. In order to simplify the diagram, a pair of dinucleotides, d(GC)<sub>2</sub>, extracted from DNA-2 is illustrated instead of the whole DNA. The DNA and AMD are drawn with open bonds and solid bonds, respectively. The initial hydrogen-bond contacts between AMD and DNA are illustrated with dashed lines.

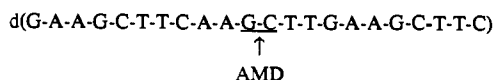
canonical A-form and B-form DNA's. The most plausible model so far built is based on the structure of DNA-2, which is shown in Figure 9. In this model, the quinoid oxygen (O3) and amino group (N2) of the phenoxazone ring interact with the amino (N2) group of the G4 residue and the oxygen atoms (O4', O5') of the C5 residue, respectively, through slightly long hydrogen bonds. There are no unusual short contacts between AMD and DNA in the model. After formation of the initial hydrogen bonds, AMD is swung around the O4' and O5' oxygen atoms of the cytosine C5 residue in order to insert the phenoxazone ring between the base pairs (see Figure 9). In the process, N2(AMD)⋯O4'(C5) and N2(AMD)⋯O5'(C5) hydrogen bonds are maintained but the O3(AMD)⋯N2(G4) hydrogen bond is broken. As mentioned previously, the *trans-trans-trans* conformation of the backbone between the G4 and C5 residues is very important for the initial contact of AMD to DNA because this unique backbone conformation brings the O5' atom to the surface of the minor groove, enabling it to become a hydrogen-bond acceptor for the amino group (N2) of AMD. This proposed intercalation process of AMD is supported by the fact that the AMD analogue, 2-chloro-AMD, replaces the amino group at the 2-position of the phenoxazone ring with chloro, does not bind to DNA, and is inactive.<sup>17</sup> In this case, the negatively charged chloro group cannot form hydrogen bonds with the negatively charged O4' and O5' atoms.

It is difficult to build an AMD approaching model based on the B-form DNA. Many unusual short contacts occur when AMD approaches the minor groove of B-form DNA to recognize the amino (N2) group of guanine and the O4' and O5' atoms with the quinoid and amino groups because the minor groove of B-form DNA is narrow and deep. It is quite obvious that AMD can recognize information more easily on a shallow and wide minor groove of A-form DNA than a deep and narrow minor groove of B-form DNA, if the initial AMD approach process is something

(45) Hamilton, L. D.; Fuller, W.; Reich, E. *Nature (London)* 1963, 198, 538-540.

similar to that proposed here. It should be noted that DNA is a very flexible molecule, and thus the B-form DNA can adopt a locally A-like conformation in solution. It has been suggested that AMD interacts with kinked B-form DNA and binds to B-form DNA<sup>46,47</sup> and does not bind to A-form DNA.<sup>45</sup> However, as described here, A-form DNA with the *trans-trans-trans* conformation of the P-O5'-C5'-C4' backbone is another possible conformation to be recognized by AMD in the initial stage of intercalation.

**Models of Longer DNA-AMD Complexes.** It is quite interesting to elucidate how the AMD changes the structure of actual long DNA by intercalatively binding to it. A model structure in which AMD binds to a longer DNA has been built on the basis of the crystal structures determined in this study. The following sequence of DNA was selected, and the AMD binding site is as shown:



Although there are some differences among the models built from complexes A, B, and C, respectively, the models based on complex C will be described here since they have the largest difference between A-form and B-form models.

The two initial models, the A-DNA model [(A-DNA):(DNA-AMD):(A-DNA)] and B-DNA model [(B-DNA):(DNA-AMD):(B-DNA)], were built by merging canonical A- and B-form DNA fragments to both ends of the complex structure determined by the X-ray analysis, respectively. After solvating the models, molecular mechanics were applied to further refine the model using the program AMBER version 4.0.<sup>35</sup> The lowest total energy structure deduced by this method is illustrated in Figure 10. The A-DNA model is a straight line model, whereas the B-DNA model is significantly kinked at the intercalation site. The refined binding site geometries in both models have a 2-fold symmetry and are quite similar to the structure of complex A.<sup>54</sup> The interaction energies between DNA and AMD are essentially the same in both models (-102 kcal *vs* -109 kcal) since the binding sites of both initial models were taken from the crystal structure. The B-DNA model gives a slightly lower total energy than the A-DNA model (-1539 kcal *vs* -1391 kcal), which is consistent with the results that the B-form DNA gives the smallest rms deviations from all complexed DNA (Table 3). Thus, the calculation suggests that AMD appears to bind the B-form DNA. However, at this level of total energy difference, we believe that we cannot predict the most likely complex structure from the calculation. This molecular modeling study indicates that we will be able to build several rational A- and B-form DNA models with docking the complex structure obtained by the X-ray study.

**AMD Binding Test.** In order to examine our hypothesis that AMD can recognize and bind to A-form DNA, an AMD binding measurement has been carried out in aqueous solution. When AMD intercalates into the DNA, the visible absorption spectrum of AMD chromophore is shifted to the longer wavelength region (red shift). Therefore, a significant difference spectrum of AMD itself and the AMD-DNA complex should be observed. It is well-known that an RNA cannot adopt the B-form conformation since the 2'-hydroxyl group of ribose would have short contacts with the phosphate group. An oligonucleotide composed of RNA fragments at both ends and a DNA fragment in the middle portion, such as r(GGG)d(AAGCTT)r(CCC), should adopt the A-form configuration, since both ends of the RNA fragments which must adopt an A-form conformation should force the middle portion of the flexible DNA oligomer to adopt an A-form conformation. If the RNA-DNA-RNA mixed oligonucleotide with AMD shows

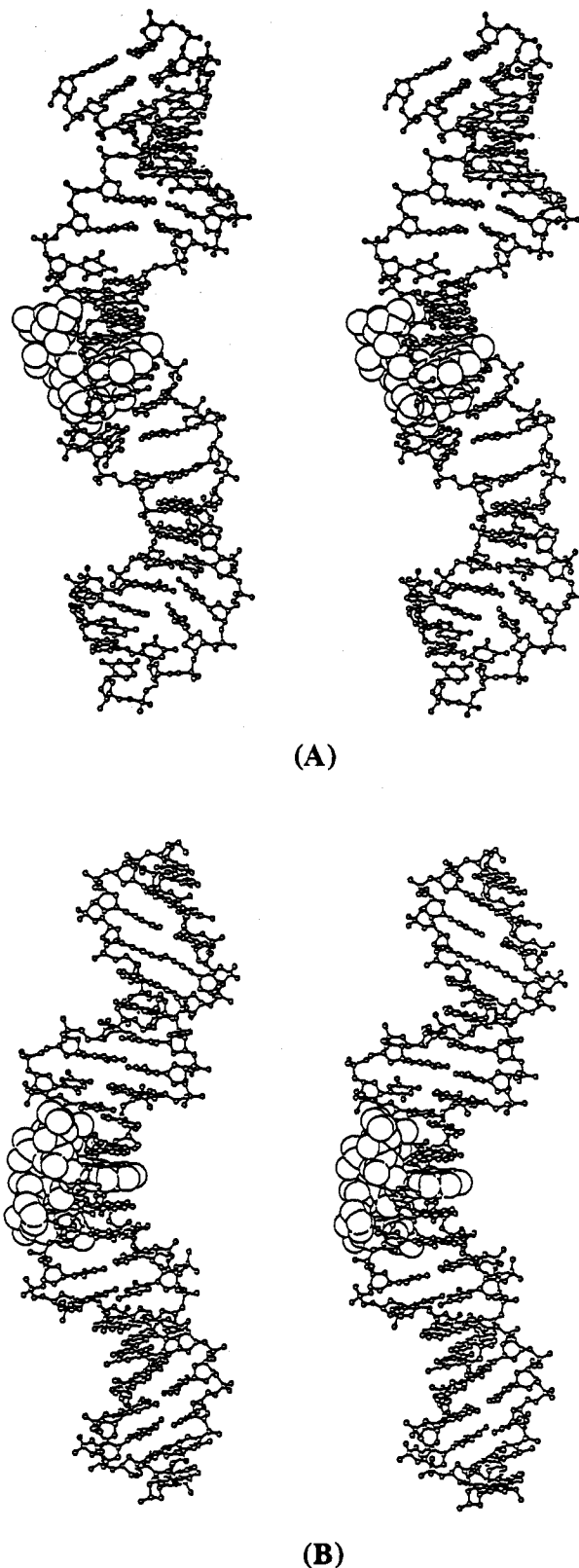


**Figure 10.** Stereo drawing of 22-mer DNA-AMD complexes refined by the AMBER calculation. The AMD molecule is illustrated with a space-fill drawing. The helical axis of the A-DNA model (A) is a straight line, whereas the helical axis of the B-DNA model (B) is significantly bent at the AMD binding site ( $\sim 30^\circ$ ).

a significant difference spectrum, then we may conclude that AMD can bind to an A-form DNA. As shown in Figure 11, the difference spectrum of r(GGG)d(AAGCTT)r(CC)d(C) is as strong as those of d(GGGAAGCTTCCC) and calf thymus DNA, suggesting that AMD does bind to the A-form DNA. It should

(46) Sobell, H. M.; Tsai, C.-C.; Jain, C.; Gilbert, S. G. *J. Mol. Biol.* 1977, 114, 333-365.

(47) Mauger, A. B.; Stuart, O. A.; Katz, E. *J. Med. Chem.* 1991, 34, 1297-1301.

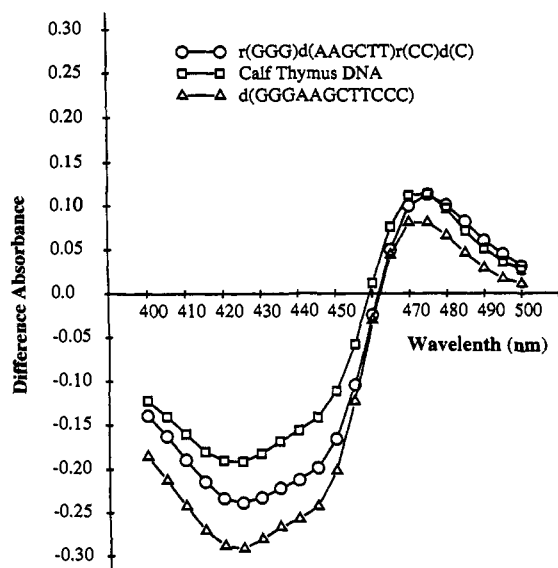


**Figure 11.** Difference spectra of AMD with r(GGG)d(AAGCTT)r(CC)d(C), d(GGGAAGCTTCCC), and calf thymus DNA.

be noted that this study does not suggest that AMD binds only to A-form DNA. As shown by fiber diffraction studies,<sup>55</sup> DNA is a quite flexible molecule found in many conformations. Thus, it is not an unusual assumption that portions of a long B-form DNA adopt partially A-like conformations and AMD's bind to those portions. It has been suggested that AMD does not bind to RNA since RNA adopts A-form conformations.<sup>48</sup> However, this study suggests that the reason why an AMD cannot intercalate into double-stranded RNA is due to steric hindrance between the O2' groups of the sugar moiety and the AMD chromophore and not due to the conformation of RNA.

### Conclusion

Three independent structures of d(GAAGCTTC)<sub>2</sub>-AMD complexes have been determined by the single crystal X-ray diffraction method. Although the structures of the complexes are similar, careful examination of the structures indicates that these three structures are significantly different but also rationally

(48) Haselkorn, R. *Science* **1964**, *143*, 682-684.

(49) Hurwitz, J.; Furth, J. J.; Malamy, M.; Alexander, M. *Proc. Natl. Acad. Sci. U.S.A.* **1962**, *48*, 1222-1223.

(50) Besler, B. H.; Merz, K. M., Jr.; Kollman, P. A. *J. Comput. Chem.* **1990**, *11*, 431-439.

(51) Stewart, J. J. P. *MOPAC, QCPE #455*, Version 5.0, 1985.

(52) Dewar, M. J. S.; Zoebisch, E. G.; Healy, E. F.; Stewart, J. J. P. *J. Am. Chem. Soc.* **1985**, *107*, 94-108.

(53) Aboul-ela, F.; Gabriele, V.; Walker, G. T.; Tinoco, I. *Nucleic Acids Res.* **1988**, *16*, 3559-3572.

(54) Huhta, D. W.; Kamitori, S.; Takusagawa, F. *Proceedings of the 35th Annual West Central States Biochemistry Conference*, Manhattan, KS, October 1992; Abstract P-21.

(55) Arnott, S.; Chandrasekaran, R.; Puigjaner, L. C.; Walker, J. K. *Jerusalem Symp. Quantum Chem. Biochem.* **1983**, *16*, 17-31.

(56) *EMBO J.* **1989**, *8*, 1-4.

related. The structures therefore represent the major conformations of the DNA-AMD complex *in vivo*. AMD is a poison to protect the microorganism from outside enemies. From the DNA-AMD complex structures, one can realize how effectively AMD has been designed by the microorganism to bind tightly to the flexible DNA molecule. It is very rare that single crystal X-ray diffraction studies find three different modes for a drug to bind to the same DNA sequence. The structural data gained in this study will be quite useful to interpret the multiple conformations of DNA-drug complexes observed by NMR studies and/or produced by the molecular mechanics and dynamics simulations.

When AMD binds intercalatively to DNA, the helix is unwound in various ways depending on factors in the binding-site environment such as hydration conditions and interactions with counterions. Also the DNA sequences around the binding site should affect the helix unwinding. An analysis of the three DNA-AMD complex structures indicates the following general pattern. When the DNA is unwound very locally, the minor groove stays relatively narrow. The cyclic depsipeptide of AMD fits into such narrow minor grooves quite well without changing the structure drastically, but the phenoxazine ring stacks mainly with the guanine. On the other hand, when the DNA is unwound by several base pairs, the minor groove becomes wide and flat. In this case, either breaking the two inter-ring hydrogen bonds by rotating the N-C $\alpha$ (Thr) bond or changing the conformation of the cyclic depsipeptide occurs in the AMD structure, in order to fit the cyclic depsipeptide into the flat minor groove. The phenoxazine ring stacks not only with guanine but also with cytosine.

The first DNA-AMD complex structure determined by the authors<sup>25</sup> was not sufficient to explain thoroughly the binding character of AMD, but now we can rationally explain the binding specificity of AMD with two additional structures of DNA-AMD complexes. A UV/vis spectroscopic study in solution suggests that AMD can bind not only to B-form DNA but also to A-form DNA. A simple molecular modeling study based on structures of DNA complexes and host DNA supports this conclusion.

**Acknowledgment.** We thank Dr. David W. Huhta for the AMBER calculation and Dr. Richard L. Schowen and Dr. David Vander Velde for critical reading of the manuscript. This research is supported by grants from the National Institutes of Health (GM-37233 and AI-28578), Kansas Health Foundation (Wichita, KS), and Marion Merrell Dow Foundation (Kansas City, MO).

**Supplementary Material Available:** Tables of positional and thermal parameters for the DNA-AMD complex and host DNA and omit maps of DNA-AMD and DNA structures (33 pages); tables of observed and calculated structure factors of the DNA-AMD complex and host DNA (10 pages). This material is contained in many libraries on microfiche, immediately follows this article in the microfilm version of the journal, and can be ordered from the ACS; see any current masthead page for ordering information. The materials have also been deposited with the Brookhaven Protein Data Bank.